

# Sparing of neuronal function postseizure with gene therapy

John McLaughlin\*, Benno Roozendaal†, Theodore Dumas\*, Anurag Gupta\*, Olusola Ajilore\*, Joseph Hsieh\*, Dora Ho\*, Matthew Lawrence\*, James L. McGaugh†, and Robert Sapolsky\*‡

\*Department of Biological Sciences, Stanford University, Stanford, CA 94305; and †Center for the Neurobiology of Learning and Memory, University of California, Irvine, CA 92697-3800

Edited by Bruce S. McEwen, The Rockefeller University, New York, NY, and approved July 25, 2000 (received for review August 17, 1999)

Numerous studies have demonstrated that gene therapy interventions can protect neurons from death after neurological insults. In nearly all such studies, however, "protection" consists of reduced neurotoxicity, with no demonstrated preservation of neuronal function. We used a herpes simplex virus-1 system to overexpress either the Glut-1 glucose transporter (GT) (to buffer energetics), or the apoptosis inhibitor Bcl-2. Both decreased hippocampal neuron loss to similar extents during excitotoxic insults *in vitro* and *in vivo*. However, the mediating mechanisms and consequences of the two interventions differed. GT overexpression attenuated early, energy-dependent facets of cell death, blocking oxygen radical accumulation. Bcl-2 expression, in contrast, blocked components of death downstream from the energetic and oxidative facets. Most importantly, GT- but not Bcl-2-mediated protection preserved hippocampal function as assessed spatial maze performance. Thus, gene therapeutic sparing of neurons from insult-induced death does not necessarily translate into sparing of function.

The mechanisms underlying neuron death after seizure, hypoglycemia, or hypoxia-ischemia all involve an excess of the excitatory neurotransmitter glutamate in the synapse. This excess causes a mobilization of free cytosolic calcium in the postsynaptic neuron, leading to calcium-dependent oxygen radical formation, cytoskeletal damage, and protein misfolding. These degenerative events ultimately result in necrotic or, in a subset of neurons, apoptotic death (1, 2).

Because such neuron death ensues over days, it is plausible to use protective gene therapy techniques during that interval. Neuroprotection has been reported in animal models of these insults with the use of neurotropic viral vectors (3, 4) overexpressing protective proteins targeting the energetic facets of damage (5–8), the calcium excess (9–11), protein misfolding (12, 13), oxygen radical production (9), apoptosis (14–19), inflammation (20, 21), or with overexpression of neurotrophins (22).

In most such studies, "protection" typically consists of reducing numbers of dead neurons or lesion size. Few studies have included *functional* endpoints, such as reducing spatial memory deficits when reducing hippocampal damage (18), or reducing motor deficits when reducing nigrostriatal damage (23, 24). In the present report, we demonstrate that a necessary further step to evaluating a gene therapy intervention is to assess its functional consequences.

## Methods

**Vectors.** Glut-1 glucose transporter (GT) was overexpressed with the herpes simplex virus (HSV)-1 amplicon vector  $\nu\alpha 4\beta\text{gal}\alpha 22\text{GT}$  (5–8), and the anti-apoptotic protein Bcl-2 with vector  $\nu\alpha 4\beta\text{gal}\alpha 22\text{bcl-2}$  (15). In these bipromoter vectors, a  $\beta$ -galactosidase ( $\beta$ -gal) reporter gene and the transgene of interest are under the control of the HSV  $\alpha 22$  and  $\alpha 4$  promoters, respectively. The two promoters are equally potent, and coexpression of the two proteins is approximately 95% (12, 13). Control vectors either contain the identical transgene with stop codons to prevent translation (Figs. 1*B*, 2*A*, 2*B*, and 3), or contain reporter gene only (Figs. 1*A* and 2*B*), producing similar results.

**Cell Culture.** Neuronal/glial cultures were prepared from hippocampi of fetal day 18 rats (Harlan Breeders, Indianapolis) (12). Cells (150,000 cells/well) were plated on 48-well plates. Cultures were 10–11 days postplating, when 50–70% of cells were non-neuronal, as assessed immunocytochemically (6, 7).

**In Vitro Neurotoxicity Studies.** Cultures were infected with indicated vector at multiplicities of infection (MOIs) of 0.8–1.1. Under these conditions and in these cultures, approximately 50% of neurons and 7% of glia are infected (unpublished data); expression first occurs at 5 h postinfection, peaks at 12, and declines by 36 (12). Sixteen hours later, cells were treated with 100  $\mu\text{M}$  kainic acid (KA; Sigma) in media containing 5 mM glucose. Neuronal viability was assessed after 8 h by staining with 3  $\mu\text{g}$  calcein AM (Molecular Probes) for 8–10 min, as per manufacturer's protocol. Neurons were identified by morphological criteria (25). Percentage dead neurons was calculated by examining five random fields/well;  $n = 12$ –13 wells/group.

**In Vivo Neurotoxicity Studies.** Adult male Sprague–Dawley rats were anesthetized and stereotaxically infused bilaterally with KA and indicated vector as follows: anterior/posterior,  $-3.3$  mm from bregma; medial/lateral,  $\pm 2.0$  mm from midline; dorsal/ventral,  $-3.5$  mm from dura (26). This infusion site corresponded to an area just dorsal to the apex of the dentate gyrus. KA (0.05  $\mu\text{g}$ ) plus indicated viral vector in 3  $\mu\text{l}$  of PBS were infused (0.5  $\mu\text{l}/\text{min}$ ). Amounts of infectious vector particles infused were as follows: GT,  $2.4 \times 10^4$ ; gts (the stop codon control for the GT vector),  $1.2 \times 10^4$ ; Bcl-2 and bst (control for the Bcl-2 vector),  $1.2 \times 10^4$ . Vector:helper ratios were 1:3–4 for GT/gts and 1:5–6 for Bcl-2/bst. No cytopathicity was observed; expression first occurs, peaks, and declines by 8, 12, and 48 h postinfection, respectively (27). Two weeks later, rats were perfused in methanol:glacial acetic acid:formaldehyde (8:1:1); brains were stored in sucrose/formalin for a week. Thirty-micrometer coronal sections through the hippocampus were cut, and every tenth one was retained. Sections were Cresyl violet-stained and examined blind at  $\times 40$  magnification. Within each section, area of damage was determined by measuring the length and width of damage with a calibrated ocular grid; this analysis produced results in agreement with counting of individual surviving neurons (28). Areas in successive sections were used to determine the total volume of damage with METAMORPH soft-

This paper was submitted directly (Track II) to the PNAS office.

Abbreviations: GT, glucose transporter; HSV, herpes simplex virus;  $\beta$ -gal,  $\beta$ -galactosidase; MOI, multiplicity of infection; KA, kainic acid; ROS, reactive oxygen species; X-Gal, 5-bromo-4-chloro-3-indolyl  $\beta$ -D-galactoside.

‡To whom reprint requests should be addressed. E-mail: sapolsky@leland.stanford.edu.

The publication costs of this article were defrayed in part by page charge payment. This article must therefore be hereby marked "advertisement" in accordance with 18 U.S.C. §1734 solely to indicate this fact.

Article published online before print: *Proc. Natl. Acad. Sci. USA*, 10.1073/pnas.210350097. Article and publication date are at [www.pnas.org/cgi/doi/10.1073/pnas.210350097](http://www.pnas.org/cgi/doi/10.1073/pnas.210350097)

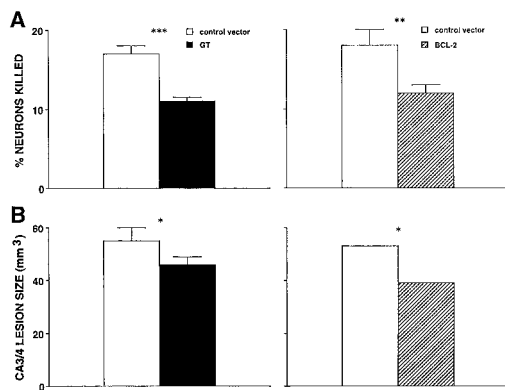


**Fig. 1.** (A) Significant reduction in KA-induced neurotoxicity in cultured hippocampal neurons by overexpression of GT (Left) or Bcl-2 (Right).  $n = 20$ –30/group. (B) Significant reduction in KA-induced hippocampal neurotoxicity by GT or Bcl-2.  $n = 10$ –15/group. \*,  $P < 0.05$ ; \*\*,  $P < 0.02$ ; \*\*\*,  $P < 0.001$ , by  $t$  test.

ware. This volumetric approach is possible because this KA dose produces a single CA3 lesion.

**Quantification of Pattern of Expression and Lesion Size.** X-Gal (5-bromo-4-chloro-3-indolyl  $\beta$ -D-galactoside)-positive puncta were counted in successive sections in rats perfused 24 h postvector. For analysis of expression in the anterior/posterior axis, counts for each hemisphere were aligned by the most anterior section that showed a defined dentate cell layer, and X-Gal-positive cells were parsed by millimeter. Positive cells/mm were divided by total positive cells to create proportion of total expression values. For analysis of expression in the medial/lateral axis, only cells in the superior blade of the dentate were counted. By using an optical grid, the superior blade was separated into three sections of equal size, and the number of X-Gal-positive cells was tallied for each third (and expressed as a percentage of the total number of X-gal-positive cells). Similar analysis was carried out in CA3 to quantify lesion patterns.

**Measurement of Reactive Oxygen Species (ROS).** ROS were measured (29) with some modifications. Cells from day 10 cultures in 12-well plates were infected with indicated vector for 24 h at an MOI of 1.0. Cells were washed once and incubated in KRPH buffer [1 mM  $\text{CaCl}_2/4.7$  mM  $\text{KCl}/1.25$  mM  $\text{MgSO}_4(\text{H}_2\text{O})/7/137$  mM  $\text{NaCl}/5$  mM  $\text{NaH}_2\text{PO}_4(\text{H}_2\text{O})/20$  mM hepes acid] (with or without 100  $\mu\text{M}$  KA, as indicated) containing 60 mM acetylcytochrome  $c$  (Sigma). After 1 h, aliquots of medium were collected and diluted with degassed distilled water. Absorption and the second derivative spectra were recorded between 500 and 600 nm against KRPH buffer diluted in water in a single-beam spectrophotometer (DU-640, Beckman). A scan speed of 2400 nm/min, with a datum point interval of 2 nm and a time constant of 2 s, was used. The second-order derivative was again recorded after the sample solutions were fully reduced by addition of sodium dithionite (Sigma). Amplitude variations were measured between the valley at 548 nm and the peak at 556 nm before and after reduction with sodium dithionite. Specific reduction of acetylcytochrome  $c$  was measured by taking the ratio of differences between the partially reduced and fully reduced sample. Ratios of reduction were standardized to protein concentration, and ROS accumulation was expressed as the percentage of mean-mock infected (without KA) values.

**Measurement of Metabolism in Cultures.** A Cytosensor (Molecular Devices) microphysiometer provided indirect measures of cellular metabolism by quantifying extracellular acidification rate

( $\mu\text{V/s}$ ) (30, 31). Cultures were prepared as indicated, and measurements were begun 20 h later. Baseline measures in 20 mM glucose (in unbuffered DMEM) were carried out for 1 h, after which cultures were switched to 0.2 mM glucose; this is time 0 in Fig. 2B.

**Maze Learning.** One week postsurgery, rats were trained and tested on a submerged platform version of the water maze and 2–4 days later on a visible platform version. The water maze was a black circular tank (diameter, 1.83 m; height, 0.58 m) filled with water (27°C) to a depth of 20 cm, and was located in a room with extramaze cues. Four starting positions were equally spaced around the perimeter of the pool. The rectangular Plexiglas escape platform used for the submerged task was submerged at a depth of 2.5 cm. For the visible platform task, a black and white striped ball (diameter, 8 cm) was attached to the submerged platform and protruded above the water surface.

In both versions of the task, rats received 1 training session consisting of six trials. On each trial, the rat was placed in the tank facing the wall at one of the four start points and allowed to escape onto the platform. If a rat did not escape within 60 s, it was manually guided to the platform. After mounting the platform, rats remained there for 20 s and were then placed in a cage for a 30-s intertrial interval. Latency to mount the platform was used as a measure of acquisition in both tasks.

In the submerged platform task, the platform was located in the same quadrant on each trial. In the visible task, the platform was placed in a different quadrant each trial. The retention test on both tasks consisted of three additional trials 48 h posttraining. For the submerged task, the platform was located in the same quadrant as during training. For the visible task, the platform was placed in a different quadrant each trial. In both tasks, latencies to mount the platform was recorded and the mean of the three trials was used as a measure of memory for the training session.

**Immunoprecipitation.** Cultures were infected with Bcl-2 or  $\beta$ -gal control vector at an MOI of 0.6 for 24 h and then lysed at 4°C with 1.0% Triton X-100 in PBS containing standard protease inhibitors. Lysates were incubated overnight with 10  $\mu\text{g}$  of anti-human Bcl-2 antibody (Dako) and then incubated with Protein G Sepharose (Amersham Pharmacia) for 2 h (4°C). Washing was done four times with Schwyzer buffer [Tris 100 mM (pH 9.0)/LiCl 500 mM/1.0% Triton X-100/1.0% 2-mercaptoethanol], then one time with PBS and one time with double distilled water. Samples were boiled with sample buffer run on 12% SDS/PAGE, transferred to a poly(vinylidene difluoride) (PVDF) (Amersham) membrane, stained with anti-human Bcl-2 (Dako) 1:500, and visualized with ECL (Amersham).

**Immunohistochemistry.** Cultures were infected with Bcl-2 vector for 24 h, fixed in methanol, and stained with anti Bcl-2 mAb 1:500 (Dako). Fluorescent conjugated secondary Abs were from Vector Laboratories.

**Statistics.** Unpaired  $t$  tests or ANOVA followed by post hoc tests were used, as indicated. Data are presented as means  $\pm$  SEMs. Absence of error bar indicates variability too small to be graphed.

## Results

As reported (6, 15), overexpression of either the Glut-1 GT or Bcl-2 protected cultured hippocampal neurons from an excitotoxin. GT and Bcl-2 reduced KA-induced damage (Fig. 1A) to similar extents (no significant difference between GT and Bcl-2 by Scheffé post hoc test after one-way ANOVA). Hippocampal microinfusion of KA in rats caused damage to CA3 pyramidal neurons. GT and Bcl-2 reduced lesion volume (Fig. 1B) to equal extents (no significant difference between GT and Bcl-2, Scheffé test).

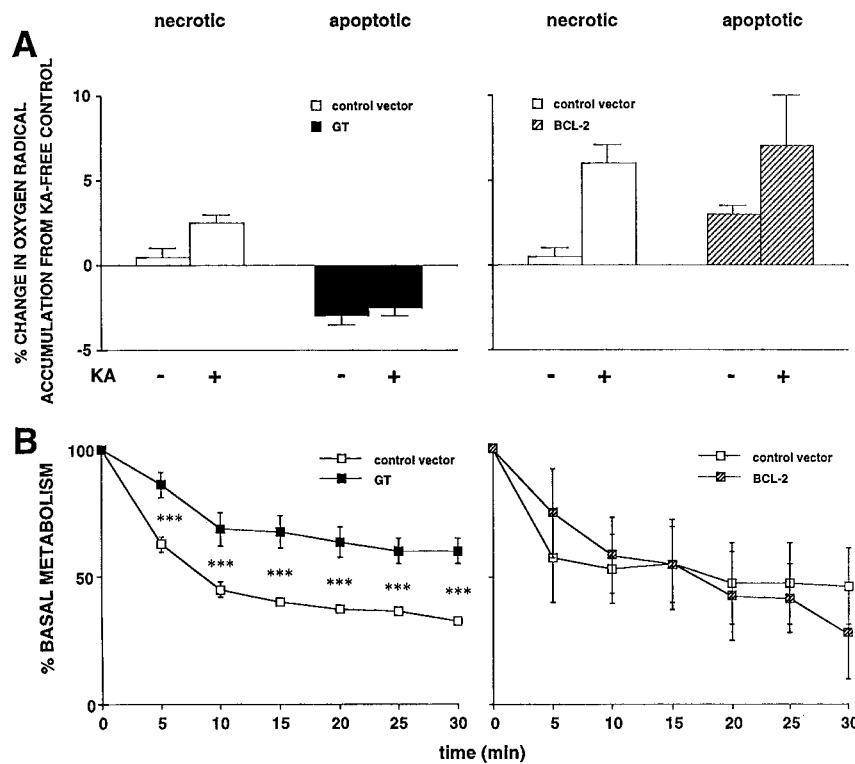


**Fig. 2.** (A) Effects of GT (Left) or Bcl-2 (Right) on ROS accumulation post-KA. Values are expressed as percentage above that in mock-infected control cultures without KA. In control vector-treated wells, KA significantly increased ROS accumulation ( $P < 0.05$  and  $0.01$  in GT and Bcl-2 studies, respectively, post hoc test after two-way ANOVA). In GT-infected wells, KA did not significantly increase accumulation, and in either condition ( $\pm$ KA), there was significantly less accumulation than in cognate control wells ( $P < 0.01$  for both). In contrast, KA significantly increased accumulation in Bcl-2-treated wells ( $P < 0.05$ ), and values did not differ significantly from the cognate control wells. (B) Effects of GT or Bcl-2 on metabolism in primary hippocampal cultures under hypoglycemic conditions as assessed by proton efflux rates, measured by microphysiometry.  $\nu$ IE1GT (Left) attenuated the drop of metabolism posthypoglycemia ( $***, P < 0.001$  by post hoc test after two-way ANOVA, comparing experimental vector versus control vector at the same time point), whereas  $\nu\alpha 22\beta gal\alpha 4bcl-2$  (Right) had no effect. Data on the left previously published (7), making use of a related HSV vector expressing either GT ( $\nu$ IE1GT) or  $\beta$ -Gal as a reporter gene ( $\nu$ IE1 $\beta$ Gal).

Having established the equivalent protective potential of these two genes by using the same vector system *in vitro* and *in vivo*, we next explored the mechanistic differences in their actions. These differences were observed in three realms. (i) We initially tested whether each transgene would still be protective if introduced post-KA. Both genes are protective when introduced within 1 h postsult *in vivo* (27, 32). In hippocampal cultures, introduction of Bcl-2 vector, but not GT, still protected 6 h post-KA survival of GT-treated cells exposed to KA:  $94 \pm 7\%$  relative to control vector exposed to KA (not significant); survival of Bcl-2-treated cells exposed to KA:  $117 \pm 6\%$ , compared with control vector exposed to KA. [ $P < 0.05$  by Scheffé post hoc test after one-way ANOVA comparing Bcl-2 with control;  $n = 60$ – $74$ /group]. This finding agrees well with a report of protective effects of an HSV-Bcl-2 vector 8 h after glutamate exposure in cortical cultures (16). (ii) We tested whether either vector protected cultures from KA-induced generation of ROS. KA increased ROS accumulation in cultures treated with control vectors (Fig. 2A), and was blocked by GT (Fig. 2A Left). However, the Bcl-2 vector, at an MOI that blocked neurotoxicity (Fig. 1), did not block ROS accumulation (Fig. 2A Right). (iii) We examined whether either vector protected cultures from KA-induced declines in metabolism. KA decreased metabolism in cultures treated with either of the control vectors (Fig. 2B). This decline was blunted by GT, as compared with its cognate control (Fig. 2B Left). However, the Bcl-2 vector, at MOI that blocked toxicity did not alter metabolism (Fig. 2B Right).

Having established different features of the protective effects of GT and Bcl-2, we explored functional consequences of their

overexpression. We determined whether GT and/or Bcl-2, which caused equivalent reductions in the volume of KA-induced hippocampal lesions, also spared cognitive function in those animals on a submerged platform test in a water maze (33).

Rats were trained in a water maze to find a submerged platform located in a fixed location surrounded by salient distal cues. KA lesions did not produce deficits during training, showing equivalent acquisition, sensorimotor, and/or motivational function (data not shown). Memory was tested 48 h later with three additional trials. Rats infused with KA and the cognate vector controls (gts or bst) had longer escape retention latencies, relative to sham-operated controls ( $P < 0.01, 0.05$ , respectively) (Fig. 3A). GT spared memory ( $P < 0.05$ ), with subjects and sham-operated rats statistically equivalent, whereas Bcl-2 did not.

When rats were trained on a visible platform task, no treatments affected training ( $F(4,335) = 1.63$ ; NS) or retention performance ( $F(4,67) = 1.05$ ; NS) (Fig. 3B). These findings further substantiate that impairments in the submerged platform task were not due to perceptual/motor deficits. Consistent with this finding is the impaired retention performance on a water-maze probe trial after CA3 damage<sup>§1</sup> (34).

Thus, despite both interventions decreasing lesion size equivalently, only the GT vector spared function. Because of this surprising finding, we examined the distribution of expression

<sup>§</sup>Roozendaal, B., Ferry, B. & McGaugh, J. (1999) *Soc. Neurosci. Abstr.* 25, 1624 (abstr.).

<sup>¶</sup>Steffenach, H., Moser, E. & Moser, M. (1999) *Soc. Neurosci. Abstr.* 25, 1622 (abstr.).



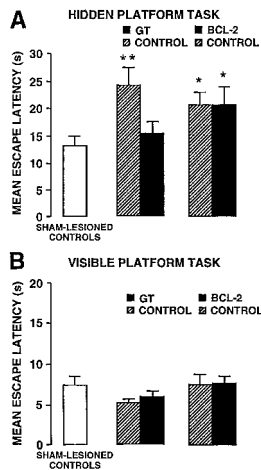


**Fig. 3.** Effects of GT (Center) and Bcl-2 (Right) on retention impairment in a submerged (A) and visible platform test (B) in a water maze produced by KA-induced lesions. Data were from the same rats used for the lesion data in Fig. 1B. \*,  $P < 0.05$ ; \*\*,  $P < 0.01$ , by post hoc test after ANOVA.

caused by the two vectors in detail, initially by quantifying transgene expression itself (i.e., GT and Bcl-2) immunohistochemically. We could readily quantify GT-positive neurons both *in vitro* and *in vivo*, as well as Bcl-2 expression *in vitro* (Fig. 4A). However, there was not sufficiently discrete Bcl-2 staining *in vivo* to quantify numbers of neurons infected (emphasized in ref. 19); this difficulty occurred despite use of different antibodies (from Dako and Santa Cruz Biotechnology), fixatives, and staining protocols, on floating or slide-fixed sections, with horseradish peroxidase or fluorescent secondary visualization. Thus, we made use of the reporter gene driven by the bipromoter transcriptional unit in our constructs, where there is more than 99% covariance in expression of the reporter gene and transgene (12). A marked covariance occurred *in vitro* between Bcl-2 and  $\beta$ -gal expression (Fig. 4B and C).

We examined the anatomical consequences of infection with the two vectors in detail. Potentially, the sparing of function by GT but not by Bcl-2 could be due to the GT vector infecting a greater number of neurons. However, it was the Bcl-2 vector that was more infective (Glut-1, 972 + 178 neurons infected; Bcl-2, 1613 + 164,  $t(16) = 2.65$ ,  $P < 0.05$  by  $t$  test;  $n = 5$ ). The GT/Bcl-2

difference might also have been due to different distributions of expression, but they did not differ in the anterior-posterior or medial-lateral plane (Fig. 5A–C). Finally, the difference might be due to different distributions of the CA3 neurons spared from KA. However, there were no such differences across two dimensions of the lesions (Fig. 5D and E). No dorsal/ventral analysis was performed because lesion of any given segment within a brain section produced complete loss of the pyramidal cell layer.

## Discussion

As reported previously, overexpression of either GT or Bcl-2 spared hippocampal neurons from excitotoxic death *in vitro* and *in vivo*. The protective effect of GT *in vitro* is commensurate with the energetic facets of necrotic insults (35, 36), and overexpression aids the costly containment of extracellular glutamate and cytosolic calcium concentrations in neurons (5–8). The protective effect of Bcl-2 *in vitro* agrees with its ability to inhibit apoptotic elements of degeneration in subsets of neurons after necrotic insults (37, 38). The transynaptic protection *in vivo* is more complex, because most neurons infected are in the dentate gyrus (3), whereas it is their target neurons in CA3 that are damaged by KA. The ability of GT to decrease glutamate release during excitotoxic insults can explain such transynaptic protection. The mechanism underlying such sparing by Bcl-2 is not clear.

More interesting were the differences between the two interventions. GT attenuated an earlier stage of the death process than did Bcl-2. GT, but not Bcl-2, spared neurons ROS accumulation, when vectors were used at a titer that decreased neuron death. The potential anti-oxidant action of Bcl-2 is controversial; some studies support such a role (39–41), others not (42, 43), and some suggest that any antioxidant effects are irrelevant to protection (44–46). We have observed that Bcl-2 caused a small reduction in ROS accumulation after exposure to a toxin that is more pro-oxidative than KA (15), suggesting a threshold of ROS load only above which Bcl-2's antioxidant effects occur. Regarding the present data, the extent of ROS accumulation post-KA was small (approximately 5%). However, because of the short-lived nature of ROS, the cumulative oxidative load would have been greater; supporting that view, a 10% increase in ROS accumulation in flies increases oxidative damage and shortens life span (47).

We also observed that GT, but not Bcl-2, buffered hippocampal cultures from the disruptive effects of KA on metabolism. This finding agrees with the finding that apoptotic pathways are

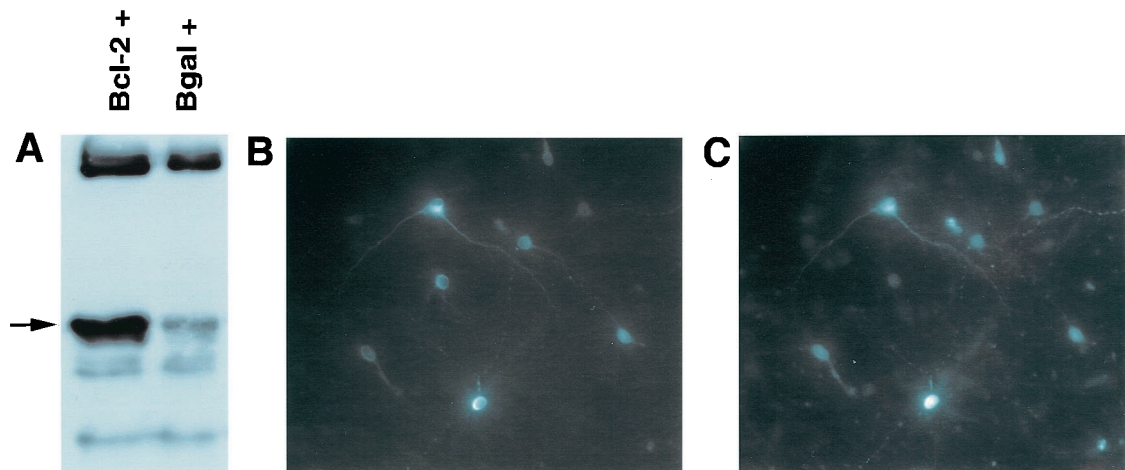


**Fig. 4.** (A) Immunoblot of immunoprecipitated cell lysates from cultures infected with Bcl-2 vector (bcl-2+) or  $\beta$ -gal control vector (Bgal+). The arrow indicates the bcl-2 protein band at approximately 30 kDa. (B and C) Cells double labeled for Bcl-2 (B) and  $\beta$ -gal (C).  $\times 200$  magnification.

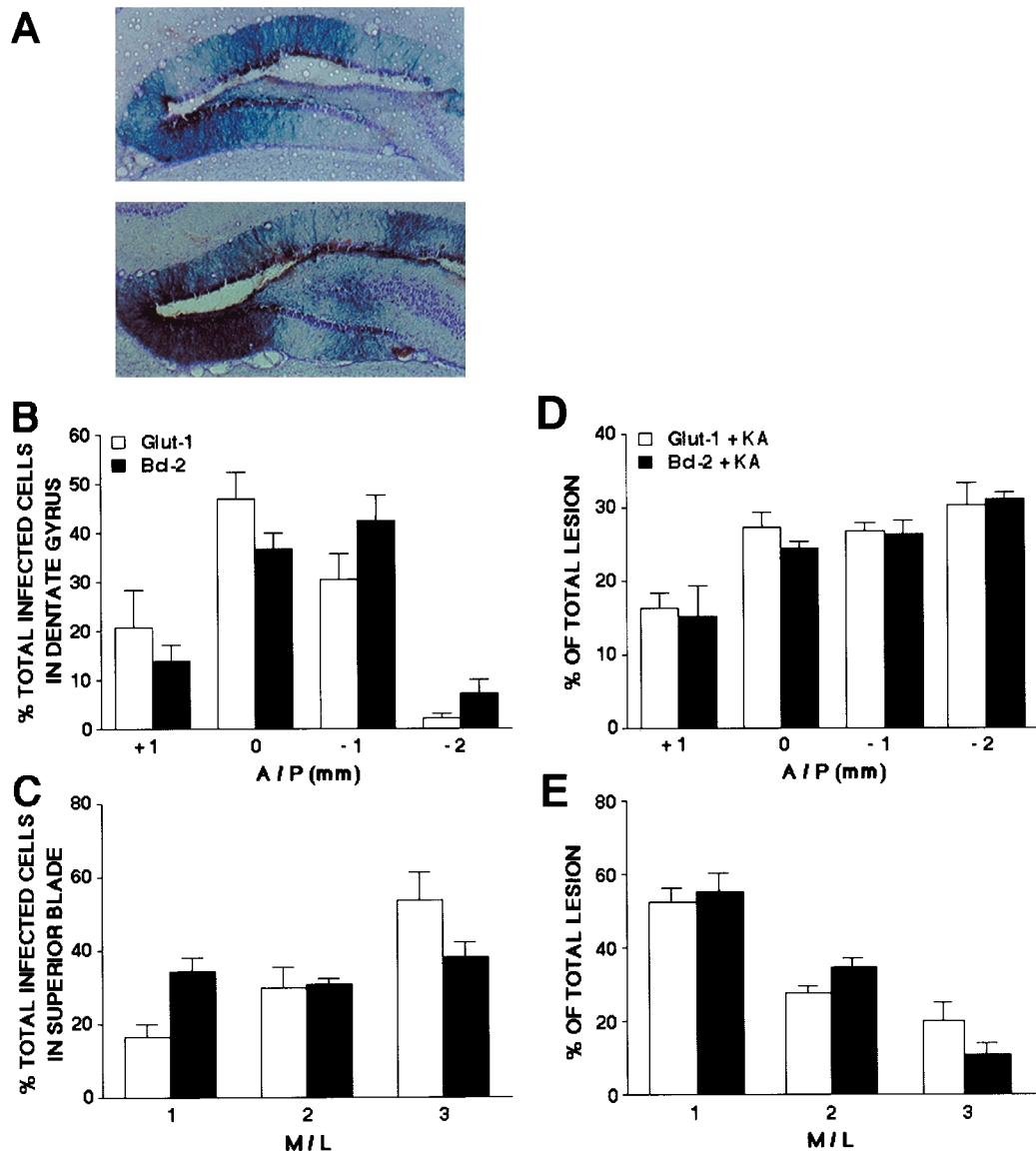


**Fig. 5.** Equivalent patterns of expression and of decreasing lesion size after treatment with GT and Bcl-2. (A) X-Gal-stained neurons ( $\times 100$ ) in representative sections (counterstained with Cresyl violet) from a rat receiving GT (Upper) or Bcl-2 (Lower). Cell bodies and large diameter dendrites of granule cells in the superior blade of the dentate gyrus are visibly stained. (B) Percentage of total X-Gal-positive cells in 1-mm regions along the anterior/posterior (A/P) axis of the dentate gyrus ( $n = 9$ /group). Mean percentage of total lesion differed between areas [ $F(3,64) = 27.23, P < 0.001$ ] but not between groups. Zero on the x axis refers to the injection site. (C) Percentage of X-Gal-positive cells on the superior blade of the dentate gyrus grouped into three equal regions along the medial/lateral (M/L) axis ( $n = 9$ /group). Mean percentage of total lesion differed between areas [ $F(2,48) = 10.01, P < 0.001$ ] but not between groups. The number "1" on the x axis refers to the most medial third. (D) Percentage of total lesion in 1-mm regions along the A/P axis for hippocampi treated with KA and Glut-1 or Bcl-2 ( $n = 5$ /group). Mean percentage of total lesion differed between areas [ $F(3,32) = 18.22, P < 0.001$ ], but not between groups. (E) Percentage of total lesion grouped into three equal regions along the M/L axis ( $n = 5$ /group). Mean percentage of total lesion differed between areas [ $F(2,24) = 51.93, P < 0.001$ ], but not between groups. The number "1" on the x axis refers to the most medial third.

activated downstream of the energy-depleting effects of necrotic insults (48). As a technical issue, the GT and Bcl-2 studies were not carried out at the same time. However, each was internally controlled and compared at the same time to its own cognate stop codon control, and cultures were infected with vector titers that reduced KA-induced toxicity.

As the most important difference between the two therapies, the GT-mediated protection produced a hippocampus that was still functional, as assessed by intact retention performance in GT-treated, but not gts-, Bcl-2-, or bst-treated, rats with seizures. The dysfunction in the Bcl-2-treated rats could reflect the energetic demands and/or the oxidative damage sustained by neurons. The neural bases of learning and memory involve an

exquisite array of cellular mechanisms (49); oxidative damage, more likely in the Bcl-2- than in the GT-treated neurons, could disrupt any number of critical steps in the process. In addition, the plasticity underlying learning is energetically costly, and substrate availability can impact the efficacy of learning and memory (50). As such, the failure of Bcl-2 to spare from the energetic consequences of KA could also have contributed to the dysfunction. Similarly, in KA-treated rats, GT, but not Bcl-2, overexpression maintains mossy fiber synaptic strength (51).

Thus, despite their similar protective effects, GT spared a functional endpoint that Bcl-2 did not. Potentially, this difference could be due to expression of GT being greater than of Bcl-2, or with a different pattern. The pattern with which lesion

size was reduced with these two vectors might also have differed in a way such that the neurons spared by Bcl-2 were less important for the particular behavioral task. However, the similar patterns of expression and reduction in lesion size argue against these possibilities.

It is unlikely that this vector system will ever be clinically practical. However, these findings have implications for neuronal gene therapy, independent of the system used. First, criteria for protection by an intervention must include broadly integrative functional endpoints, because sparing of neurons from death need not necessarily translate into sparing of function. A similar theme emerges from studies of mice with congenital motoneuron degeneration, where transgenic overexpression of Bcl-2 enhanced cell survival but did not preserve axonal integrity (52). Another implication concerns the fact that it was therapy with Bcl-2 that failed to spare function. Overexpression of a different antiapoptotic gene not only decreases neuron loss but spares behavioral deficits in a more severe model of necrotic injury (global ischemia) to a different hippocampal cell field (18). The

present data, along with our electrophysiological data (51) suggest, nonetheless, that sparing of function may be more likely with an earlier intervention targeting the energetic facets of injury. Our data suggest, counter to the prevailing bias, which favors a long time-window to allow for therapeutic intervention, that gene therapy might be most effective in saving neurons from both death and dysfunction when targeting early-stage events postinsult. While increasing the technical demands placed upon this emerging discipline, this conclusion is still salutary in the context of any gene therapy sparing neuronal function after injury.

Technical assistance was provided by R. Phillips and P. Buckmaster; manuscript assistance by T. Bliss, L. Giuli, A. Lee, L. McIntosh, M. Roy, and A. Yusim. Funding was provided by National Institutes of Health Grant RO1 NS32848 (R.S.), National Institute of Mental Health Research Grant MH 12526 (J.L.M.), Ralph W. and Leona Gerard Family Trust Postdoctoral Fellowship (B.R.), and Stanford Undergraduate Research Opportunities grants (J.H. and A.G.).

- Rothman, S. M. & Olney, J. W. (1995) *Trends Neurosci.* **18**, 57–58.
- Choi, D. (1995) *Trends Neurosci.* **18**, 58–61.
- Kaplitt, M. & Loewy, A., eds. (1995) *Viral Vectors* (Academic, New York).
- Ho, D. & Sapolsky, R. (1997) *Sci. Am.* June, 96–100.
- Ho, D., MocarSKI, E. & Sapolsky, R. (1993) *Proc. Natl. Acad. Sci. USA* **90**, 3655–3659.
- Ho, D. Y., Saydam, T. C., Fink, S. L., Lawrence, M. S. & Sapolsky, R. M. (1995) *J. Neurochem.* **65**, 842–850.
- Lawrence, M., Ho, D., Dash, R. & Sapolsky, R. (1995) *Proc. Natl. Acad. Sci. USA* **92**, 7247–7251.
- Lawrence, M. S., Sun, G. H., Kunis, D. M., Saydam, T. C., Dash, R., Ho, D. Y., Sapolsky, R. M. & Steinberg, G. K. (1996) *J. Cereb. Blood Flow Metab.* **16**, 181–187.
- Kindy, M., Yu, J., Miller, R., Roos, R. & Ghadge, O. (1996) in *Pharmacology of Cerebral Ischemia*, ed. Kriegelstein, J. (Medpharm, Stuttgart).
- Meier, T., Ho, D. & Sapolsky, R. (1997) *J. Neurochem.* **69**, 1039–1045.
- Meier, T. J., Ho, D. Y., Park, T. S. & Sapolsky, R. M. (1998) *J. Neurochem.* **71**, 1013–1020.
- Fink, S., Chang, L., Ho, D. & Sapolsky, R. (1997) *J. Neurochem.* **68**, 961–966.
- Yenari, M. A., Fink, S. L., Sun, G. H., Chang, L. K., Patel, M. K., Kunis, D. M., Onley, D., Ho, D. Y., Sapolsky, R. M. & Steinberg, G. K. (1998) *Ann. Neurol.* **44**, 584–589.
- Linnik, M., Zhos, P., Geschwind, M. & Federoff, H. (1995) *Stroke* **26**, 1670–1676.
- Lawrence, M. S., Ho, D. Y., Sun, G. H., Steinberg, G. K. & Sapolsky, R. M. (1996) *J. Neurosci.* **16**, 486–492.
- Jia, W. W., Wang, Y., Qiang, D., Tufaro, F., Remington, R. & Cynader, M. (1996) *Brain Res. Mol. Brain Res.* **42**, 350–357.
- Xu, D. G., Crocker, S. J., Doucet, J. P., St-Jean, M., Tamai, K., Hakim, A. M., Ikeda, J. E., Liston, P., Thompson, C. S., Korneluk, R. G., MacKenzie, A. & Robertson, G. S. (1997) *Nat. Med.* **3**, 997–1004.
- Xu, D., Bureau, Y., McIntyre, D. C., Nicholson, D. W., Liston, P., Zhu, Y., Fong, W. G., Crocker, S. J., Korneluk, R. G. & Robertson, G. S. (1999) *J. Neurosci.* **19**, 5026–5033.
- Antonawich, F., Federoff, H. & David, J. (1999) *Exp. Neurol.* **156**, 130–137.
- Betz, A., Yang, G. & Davidson, B. (1995) *J. Cereb. Blood Flow Metab.* **15**, 547–553.
- Hagan, P., Barks, J. D., Yabut, M., Davidson, B. L., Roessler, B. & Silverstein, F. S. (1996) *Neuroscience* **75**, 1033–1045.
- Pechan, P. A., Yoshida, T., Panahian, N., Moskowitz, M. A. & Breakefield, X. O. (1995) *NeuroReport* **6**, 669–672.
- During, M. J., Naegel, J. R., O'Malley, K. L. & Geller, A. I. (1994) *Science* **266**, 1399–1403.
- Choi-Lundberg, D. L., Lin, Q., Schallert, T., Crippens, D., Davidson, B. L., Chang, Y. N., Chiang, Y. L., Qian, J., Bardwaj, L. & Bohn, M. C. (1998) *Exp. Neurol.* **154**, 261–275.
- Banker, G. & Goslin, K. (1991) *Culturing Nerve Cells* (MIT Press, Cambridge, MA).
- Paxinos, G. (1998) *The Rat Brain in Stereotaxic Coordinates* (Academic, New York), 4th Ed.
- Lawrence, M. S., McLaughlin, J. R., Sun, G. H., Ho, D. Y., McIntosh, L., Kunis, D. M., Sapolsky, R. M. & Steinberg, G. K. (1997) *J. Cereb. Blood Flow Metab.* **17**, 740–744.
- Sapolsky, R. & Stein, B. (1989) *Neurosci. Lett.* **97**, 157–163.
- Daval, J. L., Ghersi-Egea, J. F., Oillet, J., Koziel, V. (1995) *J. Cereb. Blood Flow Metab.* **15**, 71–77.
- McConnell, H. M., Owicki, J. C., Parce, J. W., Miller, D. L., Baxter, G. T., Wada, H. G. & Pitchford, S. (1992) *Science* **257**, 1906–1912.
- Raley-Susman, K., Miller, K., Owicki, J. & Sapolsky, R. (1992) *J. Neurosci.* **12**, 773–779.
- Dash, R., Lawrence, M., Ho, D. & Sapolsky, R. (1996) *Exp. Neurol.* **137**, 43–48.
- Morris, R. (1984) *J. Neurosci. Methods* **11**, 47–56.
- Ramirez-Amay V., Escobar, M. & Bermudez-Rattoni, F. (1999) *Hippocampus* **9**, 631–636.
- Beal, M. (1992) *Ann. Neurol.* **31**, 119–130.
- Sapolsky, R. (1992) *Stress, the Aging Brain, and the Mechanisms of Neuron Death* (MIT Press, Cambridge, MA).
- Bredesen, D. (1995) *Ann. Neurol.* **38**, 839–851.
- Choi, D. (1996) *Curr. Opin. Neurobiol.* **6**, 667–672.
- Hockenbery, D. M., Oltvai, Z. N., Yin, X. M., Milliman, C. L. & Korsmeyer, S. J. (1993) *Cell* **75**, 241–251.
- Kane, D. J., Sarafian, T. A., Anton, R., Hahn, H., Gralla, E. B., Valentine, J. S., Ord, T. & Bredesen, D. E. (1993) *Science* **262**, 1274–1277.
- Hochman, A., Sternin, H., Gorodin, S., Korsmeyer, S., Ziv, I., Melamed, E. & Offen, D. (1998) *J. Neurochem.* **71**, 741–748.
- Jacobson, M. D., Burne, J. F., King, M. P., Miyashita, T., Reed, J. C. & Raff, M. C. (1993) *Nature (London)* **361**, 365–369.
- Shimizu, S., Eguchi, Y., Kosaka, H., Kamiike, W., Matsuda, H. & Tsujimoto, Y. (1995) *Nature (London)* **374**, 811–813.
- Adams, J. & Cory, S. (1998) *Science* **281**, 1322–1326.
- Green, D. & Reed, J. (1998) *Science* **281**, 1309–1315.
- Gardner, A., Xu, F., Fady, C., Sarafian, T., Tu, Y. & Lichtenstein, A. (1997) *Cell Death Differ.* **4**, 487–495.
- Sohal, R. & Dubey, A. (1994) *Free Radical Biol. Med.* **16**, 621–626.
- Marton, A., Mihalik, R., Bratincsak, A., Adleff, V., Petak, I., Vegh, M., Bauer, P. I. & Krajcsi, P. (1997) *Eur. J. Biochem.* **250**, 467–475.
- Bailey, C., Bartsch, S. & Kandel, E. (1996) *Proc. Natl. Acad. Sci. USA* **93**, 13445–13449.
- Gold, P. (1995) *Am. J. Clin. Nutr.* **61**, 987S–989S.
- Dumas, T., McLaughlin, J., Ho, D., Lawrence, M. & Sapolsky, R. (2000) *Exp. Neurol.*, in press.
- Sagot, Y., Dubois-Dauphin, M., Tan, S. A., de Bilbao, F., Aebischer, P., Martinou, J. C. & Kato, A. C. (1995) *J. Neurosci.* **15**, 7727–7733.